

A study of the long-term activity of five intermediate polars with accretion discs

Vojtěch Šimon^{1,2}★

- ¹Astronomical Institute of the Czech Academy of Sciences, 25165 Ondřejov, Czech Republic
- ²Czech Technical University in Prague, Faculty of Electrical Engineering, 16627 Prague, Czech Republic

Accepted 2021 March 9. Received 2021 March 6; in original form 2020 May 26

ABSTRACT

Intermediate polars (IPs) are cataclysmic variables with mildly magnetized white dwarfs (WDs). This analysis of the long-term optical activity of five examples of IPs with accretion discs used data from the Catalina Real-time Transient Survey, Digital Access to a Sky Century @ Harvard (DASCH) and the American Association of Variable Star Observers (AAVSO). It is shown that each of these IPs had their most preferred value of absolute magnitude $M_{\rm opt}$, even if it significantly varied on the superorbital time-scale. The values of $M_{\rm opt}$ of these IPs were in the zone of thermal-viscous instability (TVI) of the disc most of the time. The properties of a series of outbursts of V426 Oph can be explained by an intermittently operating TVI. The activity of TV Col and DW Cnc is interpreted as caused by a gradually variable mass inflow rate from the secondary to a cool disc. The mass transfer rate from the secondary varied on a well-determined time-scale. It is shown that $M_{\rm opt}$ of EI UMa, close to the peaks of outbursts of non-magnetic dwarf novae, fluctuated on the time-scale of days; it also produced short flares, ascribed to the bursts of matter from the donor. HY Leo, with a presumably cool disc, fluctuated between its high and low states. A temporary brightening from an extended low state is ascribed to a short, intense burst of matter from the donor to the remaining cool disc or torus.

Key words: accretion, accretion discs – magnetic fields – radiation mechanisms: general – circumstellar matter – novae, cataclysmic variables – white dwarfs.

1 INTRODUCTION

Cataclysmic variables (CVs) are binaries with an orbital period $P_{\rm orb}$ typically of hours. Matter transfers on to the white dwarf (WD) from its lobe-filling companion (see Warner 1995 for a review). The factor that separates magnetic CVs from non-magnetic CVs (nCVs) is the strength B of this WD's magnetic field. This field strongly affects the flow and structure of the transferring matter.

The strong magnetic fields of the WDs in some CVs that are called polars strongly influence the mass flow (Cropper 1990) and cause strong polarization of their optical emission (Krzeminski & Serkowski 1977; Tapia 1977). The matter flows directly toward the magnetic poles of the WD, synchronously spinning with $P_{\rm orb}$. No accretion disc can be formed (Cropper 1990). The observed activity of polars comes from the emission produced by several processes in a small accretion region on the WD (Kuulkers et al. 2006). Cyclotron emission is dominant in the optical band while bremsstrahlung dominates the medium and hard X-ray emission (with energy E even larger than 20 keV). Variations of the mass transfer rate from the donor (secondary) to the WD, \dot{m} , govern the activity of polars, mainly consisting of high and low states (e.g. Hessman, Gänsicke & Mattei 2000; Kafka & Honeycutt 2005).

In CVs with mildly magnetized WDs (*B* of several megagauss), so-called intermediate polars (IPs; Warner & McGraw 1981; Warner 1995), the accretion disc can be present, but the magnetic field of the WD truncates its inner region. The accretion flow of the IP is

controlled by the WD's magnetic field inside the magnetosphere (Alfvén radius) of this accretor. Accretion curtains connecting the inner disc region and the accreting regions at the WD's magnetic poles (polar caps) cause an almost radial inflow on to the WD (Norton & Watson 1989; Norton 1993; Warner 1995). Thermal emission of the accretion disc dominates in the optical and ultraviolet (UV) regions. Bremsstrahlung X-ray emission comes from the accretion columns at the polar caps. The spin periods of their WDs, $P_{\rm sp}$, are shorter than their $P_{\rm orb}$ (e.g. Patterson & Price 1981). Some IPs are disc-less: much of the accretion flow in V2400 Oph is not in a coherent stream but is circling the WD, possibly as a ring of blobs (Hellier & Beardmore 2002).

Currently, a CV should be multiperiodic and a hard X-ray emitter to be classified as an IP (Warner & McGraw 1981; Warner 1995). The presence of two periods in the observed emission is essential in this regard. The longer period is attributed to $P_{\rm orb}$ or the beat period, the shorter period to $P_{\rm sp}$ of the WD or the beat period (e.g. Buckley et al. 1995). The X-ray spectrum properties can also suggest an IP nature, even in CVs with closely aligned magnetic and spin axes of the WD. This close alignment would not provide a detectable modulation with $P_{\rm sp}$. Baskill, Wheatley & Osborne (2005) studied the hardness ratios of various CVs using the *Advanced Satellite for Cosmology and Astrophysics (ASCA)* Gas Imaging Spectrometer (GIS), and they found that some CVs possess exceptionally hard X-ray spectra. They argued for reclassifying V426 Oph, for example, as an IP based on this spectral property.

CVs that exchange matter between certain limits of \dot{m} to the accretion disc are subject to this disc's thermal-viscous instability (TVI; Smak 1984; Hameury et al. 1998). They are called dwarf

^{*} E-mail: simon@asu.cas.cz

Table 1. Parameters of IPs used in this study. The lengths of $P_{\rm orb}$ and $P_{\rm sp}$ are measured in hours. The value $P_{\rm sp}/P_{\rm orb}$ gives the ratio of both periods. Distance is denoted as d. The values of d, given in parsec, were determined from the observations by the European Space Agency (ESA) *Gaia*. Extinction measured in magnitudes is abbreviated as A_V . IPs are ordered based on their right ascensions. The references cited are: He93, Hellier (1993a); Ra04, Rana et al. (2004); Ro04, Rodríguez-Gil et al. (2004); Pa04, Patterson et al. (2004); Th86, Thorstensen (1986); Re08, Reimer et al. (2008); Ro05, Rodríguez-Gil et al. (2005); He88, Hessman (1988); Ba05, Baskill et al. (2005); Pa89, van Paradijs, Kraakman & van Amerongen (1989); Pa79, Patterson (1979).

Name	P_{orb} (h)	$P_{\rm sp}$ (h)	$P_{\rm sp}/P_{\rm orb}$	d (pc)	A_V
TV Col	5.4864 (He93)	0.53050 (Ra04)	0.09669	505 ± 5	0.09
DW Cnc	1.43496 (Ro04)	0.64306 (Pa04)	0.44814	208 ± 3	0.03
EI UMa	6.4344 (Th86)	0.20717 (Re08)	0.03220	1095 ± 43	0.10
HY Leo	4.125 (Ro05)	1.15285 (Ro05)	0.27948	1151 ± 139	0.13
V426 Oph	6.847536 (He88)	0.48667? (Ba05)		191 ± 2	0.12

novae (DNe) (see Warner 1995 for a definition). Even some IPs with accretion discs (although with the missing inner disc region caused by the magnetic field of the WD) can still show the DN outbursts (Hameury & Lasota 2017). The changes in \dot{m} , governed by the outflow from the donor, can cause the low states in IPs, whether they accrete via a disc or not.

The observable outcome of the modalities in the transferring matter is governed by the following processes: the TVI of the accretion disc (Smak 1984; Hameury et al. 1998) causing the outbursts of DNe with the time-scale of days, weeks or months; changes of \dot{m} (high and low states in nova-like CVs and polars, with the time-scale of days, weeks, months or years; Livio & Pringle 1994).

This paper investigates the long-term activity of an ensemble of five IPs in the optical band. The choice of these IPs is based on the transfer of matter on to the magnetized WD via the accretion disc and the existence of the long, densely populated time segments of their observations. A preliminary version of part of this analysis was presented by Šimon (2015).

2 OBSERVATIONS

The Catalina Real-time Transient Survey (CRTS; Drake et al. 2009) obtained CCD images of IPs in the *V* band between the years 2005 and 2013.

A set of the *V*-band CCD data (sometimes supplemented by the *CV* band observations) was obtained also from the American Association of Variable Star Observers (AAVSO) International Data base³ (Kafka 2018).

The digitized photographic data were obtained from the Digital Access to a Sky Century @ Harvard (DASCH;⁴ Grindlay & Griffin 2012; Grindlay et al. 2012). This data base provides SEXTRACTOR-based photometry of every resolved object.

3 DATA ANALYSIS

A list of IPs used for this study is given in Table 1. It contains five objects for which observations of the long-term activity in the time segments of years are available. The distance d of each IP was determined from the observations made by the satellite *Gaia* (Brown et al. 2018; Bailer-Jones et al. 2018).

Table 2p gives the observing log. The observations of most IPs come from the CRTS data base. Between one and eight images (typically four, separated by several minutes or tens of minutes) of a given object were obtained per night. Although this number of images was too low to study the light curves of rapid changes (e.g. on the time-scale of minutes), we could estimate how much such changes affected the light curves of IPs on the time-scale of days and longer. Also, the means of brightness from the data points obtained in a given night were calculated. This approach also enabled us to calculate the standard deviation of the brightness of such a night mean. We found that the scatter of the individual observations obtained in the time segment of about 46 min in a given night is smaller than that occurring on longer time-scales (e.g. days and weeks). The night means thus provide a good representation of the light curve on long time-scales.

3.1 Absolute optical magnitudes of IPs

Fig. 1 shows the relation of $P_{\rm orb}$ and absolute optical magnitudes $M_{\rm opt}$ of the IPs included in this analysis. The typical mean, minimum and maximum magnitude (see Sections 3.2–3.6 for details) of a given IP, determined only from the light curves used in this study, are displayed.

These values of M_{opt} were determined for the values of d, listed in Table 1. Extinction A_V was determined from the three-dimensional (3D) map of Galactic reddening⁶ by Green et al. (2018).

Most CCD observations in this study were obtained in the V band. The photographic data band (older than the CCD observations) can be approximated by the B band. Indeed, we compared the B-band measurements with those of the V band. Still, the peak-topeak amplitude of the brightness variations was considerably higher than the possible changes of the colour indices. These indices only slightly modified $M_{\rm opt}$ of these IPs. The colour variations were thus not expected to influence Fig. 1 dramatically.

A relation between $P_{\rm orb}$ and the peak magnitude of outbursts of the presumably non-magnetic DNe (according to Patterson 2011) is included in Fig. 1. The *V*-band absolute magnitudes of the secondary (donor) stars are from equation (2.102) of Warner (1995).

3.2 TV Col

TV Col is classified as an IP because it displays several periods: P_{orb} of 5.4864 h, P_{sp} of 0.5305 h, a superhump period of 6.3 h and a beat period of 96.576 h (Hutchings et al. 1981; Schrijver et al. 1985; Retter et al. 2003; Rana et al. 2004). TV Col has an accretion disc

¹http://crts.caltech.edu/

²http://nesssi.cacr.caltech.edu/cgi-bin/getcssconedbid_release2.cgi#simtable

³https://www.aavso.org/data-download

⁴http://dasch.rc.fas.harvard.edu/lightcurve.php

⁵http://vizier.cfa.harvard.edu/viz-bin/VizieR?-source=I/347

⁶http://argonaut.skymaps.info/

Table 2. Observing log of IPs. The data bases, detectors and bands are given in Section 2. DASH (L) gives the observations of EI UMa below the plate limit. Err. gives the errors of the brightness of IPs on the images. Start of observing, T_{start} , is given in JD 240 0000. The duration of the time interval between the start and the end of observing is abbreviated as Δt (d). No.obs. gives the number of observations during the whole time segment. No.nights represents the number of observing nights. No.obs.night gives the number of images on a given night. The separation of the individual images in a given night is marked as S (in d).

Name	Data base Detector	Band	Err. (mag)	$T_{ m start}$	Δt	No.obs.	No.nights	No.obs.night	S
TV Col	CRTS CCD	V	0.06 (0.05-0.20)	53 600	2807	284	78	1–5 (4)	0.0040-0.0451 (0.0088)
DW Cnc	CRTS CCD	V	0.06 (0.06-0.12)	53 469	3127	416	104	1-8 (4)	0.0003-0.0167 (0.0055)
EI UMa	DASH plates	B	0.25 (0.05-0.34)	13 659	33 878	394	324	1-4(1)	0.001-0.143 (0.038)
EI UMa	DASH plates	B		12 552	35 090	2571	1753	1–9 (1)	0.0003-0.6598 (0.0350)
	(L)								
EI UMa	CRTS CCD	V	0.06 (0.05-0.07)	53714	2875	265	68	1-5 (4)	0.0032-0.0178 (0.0062)
HY Leo	CRTS CCD	V	0.08 (0.06-0.29)	53 500	3096	453	113	1-8 (4)	0.0005-0.0471 (0.0054)
V426 Opl	hAAVSO CCD	V	0.014 (0.002-0.18)	55 596	2469	10 088	1150	1-588	1-d means

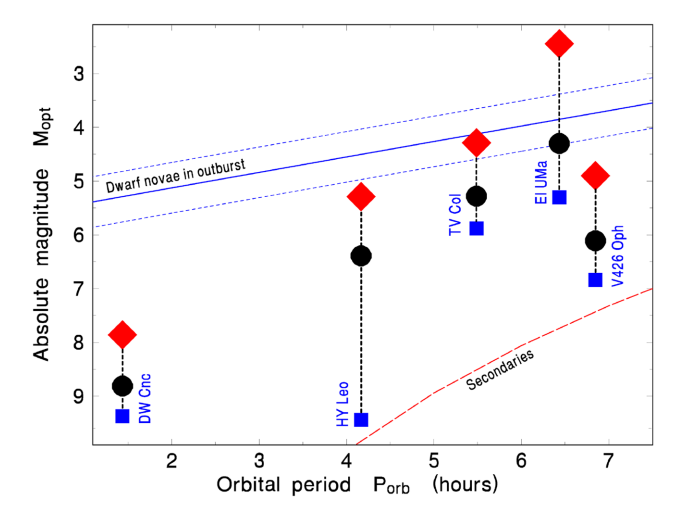


Figure 1. Absolute magnitudes $M_{\rm opt}$ of the IPs versus their $P_{\rm orb}$. The filled diamonds mark the observed peaks of brightness (e.g. outbursts, flares). The filled squares denote the lowest states. The filled circles show $M_{\rm opt}$ of the typical high states or the base of some outbursts (as explained in the text). The solid blue line represents maxima's peaks (not supermaxima) of outbursts of DNe (Patterson 2011). The dashed lines denote the standard deviation. The V-band absolute magnitudes of the secondaries are from Warner (1995). See Section 3.1 for details.

because it obeys the well-known relation between superhump period excess and P_{orb} (Retter et al. 2003).

A UV/optical flare of TV Col was detected by Szkody & Mateo (1984). Hellier & Buckley (1993) suggest that another outburst of TV Col was caused by a burst of the mass transfer from the secondary, not by the TVI of the accretion disc. These outbursts of TV Col might be relatively frequent because they were observed by Szkody & Mateo (1984), Schwarz & Heemskerk (1987), Augusteijn et al. (1994), Hellier & Buckley (1993), Hudec, Šimon & Skalický (2005). The outburst duration is of the order of days or even shorter (Augusteijn et al. 1994).

The observations in Fig. 2 come from the CRTS data base. The means of brightness from the data points obtained in a given night (in the time segment of at most about $0.2255\,\mathrm{d}$ from Table 2), mag_{av} , reveal that the scatter of these individual observations was smaller than that occurring on the longer time-scales (e.g. days and weeks).

The value of mag_{av} and its standard deviation σ_{mag} were calculated for each night mean. All these values of σ_{mag} were then plotted as a function of mag_{av} (Fig. 3). Their analysis revealed no convincing

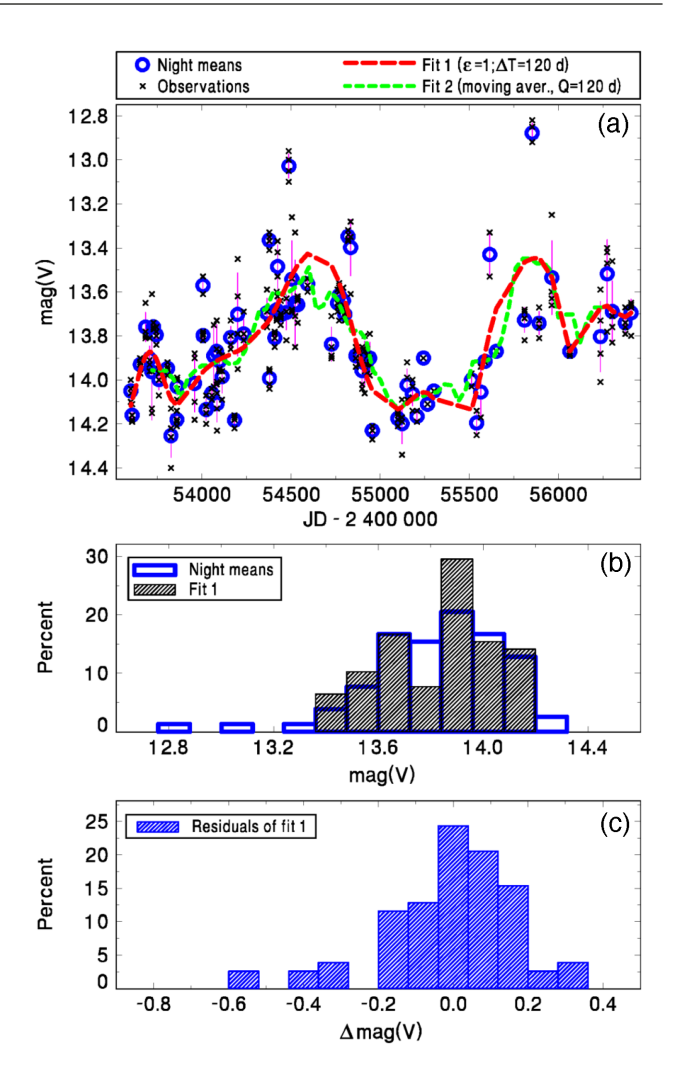


Figure 2. (a) The long-term optical activity of TV Col (the CRTS data). The legend gives the meaning of the symbols and the fits. The lines mark the standard deviations of the brightness of the night means. (b) Histograms of brightness from panel (a) (both for the night means and for fit 1). (c) Histogram of the residuals of fit 1. Notice the long tail toward the negative values of $\Delta \text{mag}(V)$. See Section 3.2 for details.

mutual dependence. Therefore, the variations of the peak-to-peak amplitude of $\sigma_{\rm mag}$ did not cause the changes of $mag_{\rm av}$ in the long-term light curve. This result is important because the light curve in Fig. 2 shows features like flares or bumps. The peak-to-peak

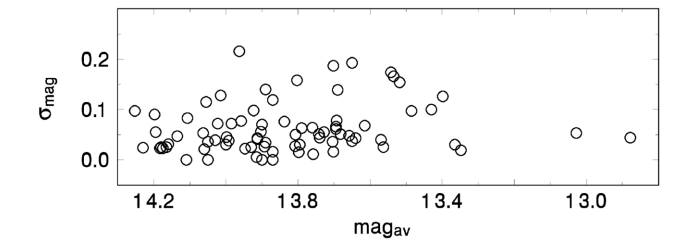


Figure 3. Relation between mag_{av} and σ_{mag} in TV Col, using the CRTS data from Fig. 2. See Section 3.2 for details.

amplitude of intranight brightness variations was lower than that of the long-term changes. The short time variability did not depend on the magnitude of TV Col. The night means in Fig. 2 thus provide a reliable representation of the light curve on long time-scales.

To separate the long-term evolution of TV Col from its shorter-term (outbursting) activity, the light curve consisting of the night means was smoothed by the code HEC13, written by Professor P. Harmanec ⁷ (Harmanec 1992) and based on the method of Vondrák (1969). It can fit a smooth curve to non-equidistant data, no matter what their profile is. A full description can be found in Vondrák (1969). HEC13 makes use of two input parameters, ϵ (in dimensionless units) and ΔT (in d in our case). The quantity ϵ determines how 'tight' the fit will be, that is, if only the main profile or also the high-frequency variations are to be reproduced. The quantity ΔT is the time interval over which the data are binned before smoothing. This method enables us to find a compromise between a curve running through all the observed points and an ideal smooth curve.

A set of the HEC13 fits of the night means of brightness of TV Col was generated and submitted for inspection. First, we investigated the role of the different values of ϵ in fitting the data. A comparison of the histogram of brightness for $\epsilon=1$, $\Delta T=60\,\mathrm{d}$ with the histograms for $\epsilon=10^{-9}$, $\Delta T=60\,\mathrm{d}$ and $\epsilon=10^{9}$, $\Delta T=60\,\mathrm{d}$ revealed no differences among them. Therefore, we varied ΔT . We found that the interval over which the data were binned before smoothing influenced the contribution of the relatively rapid (several days) variations of brightness to this fitted curve. In conclusion, the HEC13 fits for various values of ΔT revealed a dominant wave with the maxima of brightness separated by about $1000\,\mathrm{d}$ (Fig. 2a).

We also compared the result of the HEC13 fit and a smoothing of the night means by the two-sided moving averages (MA) with various filter half-widths Q (Fig. 2a). This method was described in Brockwell & Davis (1987). Although the MA fit with $Q=120\,\mathrm{d}$ was less smooth than the HEC13 fit to the data, they provided mutually similar results. This agreement confirmed the result of HEC13.

A histogram of mag_{av} in Fig. 2(b) shows a single broad bump (spanning the square and the circle in Fig. 1) with a long tail towards a higher brightness (the diamond in Fig. 1 representing the peaks of the flares). The histogram for fit 1 shows that the fitting removed this tail and influenced the bump's peak. It is mildly bimodal now. This shape is caused by a wave with two observed peaks of the light curve, separated by about 1000 d.

Fig. 2(c) shows an asymmetric histogram of the residuals of fit 1, Δ mag(V). A long tail toward the negative values of Δ mag(V) can be explained as the short flares (outbursts). Their lengths are mainly given by the scatter of the night means of the closely spaced nights in the light curve in Fig. 2(a).

A segment of the light curve of one such outburst is shown in fig. 1 of Retter et al. (2003) (not included in Fig. 2). Although the values of $M_{\rm opt}$ in Fig. 1 mean that TV Col is situated in the region of the TVI of the disc, Hellier & Buckley (1993) interpreted an outburst (not in the time of our observations) of TV Col as a mass transfer event because of the spectral variations. The outburst was a mass transfer burst also in the model of Hameury & Lasota (2017).

In the interpretation, the mass transfer rate from the secondary varies on a well-determined time-scale. We ascribe a cycle with the length of about 1000 d (Fig. 2a; with $M_{\rm opt}$ between the square and the circle in Fig. 1) to a gradually variable mass inflow from the donor to a cool disc. The superimposed optical outbursts (the diamonds in Fig. 1) can be attributed to the extreme cases of fluctuations of the outflow. Regarding the short brightenings superimposed on this cycle, the model of Hameury & Lasota (2017) shows that a brightening caused by a burst of mass transfer can be short with a steep decay if the disc remains in the cool state. The hotspot's optical emission, where the stream collides with such a disc, dominates during the outburst. In contrast, a burst of the mass transfer on to an ionized disc would cause a much slower decay (more than about 10 d) of the outburst's optical emission. Although some bursts of TV Col reached the peak magnitudes of some outbursts of the presumably non-magnetic DNe (Fig. 1), the steep decays of these bursts in this IP (less than about 1 d) suggest that even these bursts of the mass transfer did not switch the disc to a hot (ionized) state.

3.3 DW Cnc

DW Cnc is an IP because of its multiple periodicities. Uemura et al. (2002) found kilosec quasi-periodic oscillations (QPOs) in DW Cnc during a bright state ($R_c \approx 14.7$) for 61 d. A period analysis yielded a power spectrum with two peaks of QPOs (0.6250 and 1.2233 h). An investigation of the radial velocities of Patterson et al. (2004) yielded strong detections at two periods, 1.4350 and 0.6431 h, interpreted as $P_{\rm orb}$ and $P_{\rm spin}$ of a magnetized WD. Patterson et al. (2004) interpreted the spectra as the emission of the accretion disc and its interaction with the stream. Nucita, Conversi & Licchelli (2019) studied the 0.3–10 keV light curves. They confirmed the period at 0.633 h. In the optical monitor (OM) light curve, they found a signature for a period at 1.25 \pm 0.35 h, consistent with both the orbital and spin-orbit beat. Rodríguez-Gil et al. (2004) showed a double-peaked profile of the Balmer and He I lines, indicating the presence of the accretion disc.

Various interpretations of the complicated light curve of DW Cnc have been suggested. Stepanyan (1982) detected the brightness variations of DW Cnc as between 15 and 17.5 mag, and considered it a DN. However, Uemura et al. (2002) proposed that DW Cnc is a nova-like variable; this was supported by Rodríguez-Gil et al. (2004). They claimed that the long-term behaviour of DW Cnc resembled that of the VY Scl CVs. Its typical brightness of mag(V) was 14–15, occasionally decreasing to at least mag(V) \approx 16. These low states were the repeating events; the last event, with a decrease to mag(V) \approx 17.5, occurred in 2018–2019 (Segura, Ramírez & Echevarría 2020). The activity of DW Cnc was even more complicated because Crawford et al. (2008) observed an outburst on 2007 January 25. This event represented a brightening of about 4 mag from both recent measurements and long-term average quiescence.

The long-term optical activity (the CRTS data) of DW Cnc is shown in Fig. 4. The light curve, made of the night means, was smoothed by the HEC13 code (see Section 3.2). This approach is analogous to that for TV Col in Section 3.2. A set of the HEC13 fits revealed the role of the different values of ΔT also for DW Cnc.

The fit in Fig. 4(a) shows several transitions with an amplitude higher than 1 mag. Also, several waves longer than 100 d are visible,

⁷http://astro.troja.mff.cuni.cz/ftp/hec/HEC13/

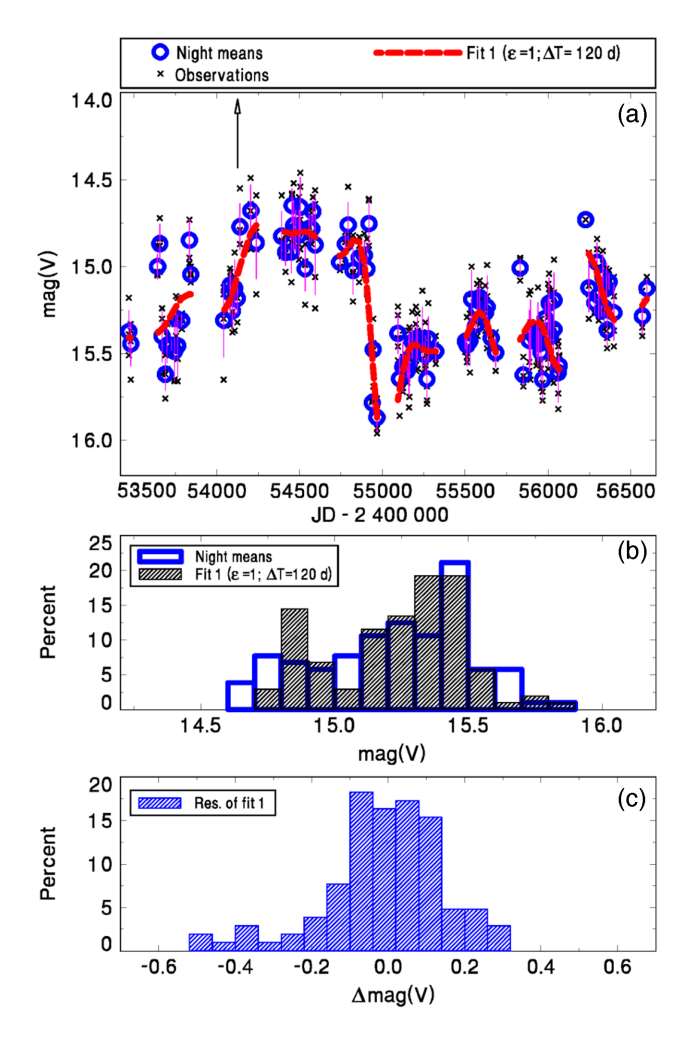


Figure 4. (a) The long-term optical activity of DW Cnc (the CRTS data). The legend gives the meaning of the symbols and the fit. The lines mark the standard deviations of the brightness of the night means. A solid vertical line denotes the position of an outburst in 2007. (b) Histograms of brightness (both for the night means of the data and for the HEC13 fit). (c) Histogram of brightness of the residuals of the fit, Δ mag(V). See Section 3.3 for details.

with the peak-to-peak amplitude lower than that of the night-to-night changes. Although the HEC13 fit in Fig. 4(a) shows a steep decline from a long bump (plateau) near JD 245 5000, this transition finished in a considerably brighter state than the deep low states (as low as about 17.5 mag), detected by Stepanyan (1982) and Segura et al. (2020) at other times.

A histogram of the brightness of the night means in Fig. 4(b) shows a broad, asymmetric bump with a tail towards a higher brightness. This range of brightnesses corresponds to the region between the square and the diamond in Fig. 1. The circle in Fig. 1 denotes the peak of the bump in the histogram in Fig. 4(b). The CRTS observations captured DW Cnc residing deep in the region of the TVI of the accretion discs.

The histograms in Fig. 4(b) also show a second peak near the brightness $14.8 \,\mathrm{mag}(V)$ (prominent especially in the HEC13 fit). It corresponds to a plateau starting near JD 245 4000 and finishing by a steep drop near JD 245 5000. We interpret this plateau as a transient (several hundreds of days) increase of the donor's mass outflow rate to a cool, low-viscosity disc. This is suggested by M_{opt} of DW Cnc deep in the region of the TVI (Fig. 1).

Although the outburst of Crawford et al. (2008) occurred in a gap of the CRTS observations, it occurred during the rise to this plateau. In the model of Lasota, Hameury & Hure (1995), this increase of the mass inflow rate to the disc from the donor could increase the disc's column density closer to the transition between the cool and the hot state. Heating and cooling fronts (Smak 1984; Hameury et al. 1998) could traverse the disc and give rise to a DN outburst. Because of its short duration, this was a normal outburst, not a superoutburst. A steep drop of brightness near JD 245 5000 (the finish of the plateau) can be caused by a decrease of the mass inflow rate to a cool disc.

We ascribe the tail towards higher Δ mag(V) in the histogram in Fig. 4(c) to the short flares. The light-curve coverage shows that the duration of such a flare is at most several days. The bursts of mass outflow from the donor to the lobe of the WD can produce such short optical bursts if they are caused by the collisions of the stream and the cool, low-viscosity disc in the hotspot (see the model of Hameury & Lasota 2017).

3.4 EI UMa

EI UMa was classified as an IP according to its X-ray spectra (Pandel 2004) and the spin modulation of the WD (0.20717 h) in the optical band (Reimer et al. 2008; Kozhevnikov 2010). Thorstensen (1986) showed that the optical spectrum of EI UMa is consistent with that of the accretion disc.

Fig. 5 shows a relatively stable optical brightness, usually with only small fluctuations (about 1 mag) on the superorbital time-scales. Only the best DASCH observations without plate defects, and with errors of the brightness of EI UMa smaller than 0.35 mag, were used. The plates with EI UMa below the plate limit were used for constraining its brightness.

The colour index B-V close to 0 (Reimer et al. 2008) enabled us to compare the brightness of EI UMa in the B and V bands. Although the DASCH data may be subject to systematic errors due to specific image quality problems, the most important finding is a very long (decades) state of a very high $M_{\rm opt}$ of EI UMa.

Besides the fluctuations of brightness, several short outbursts (or flares) with a peak magnitude higher than 13.5 mag(*B*) were also detected. The plates obtained in the surrounding nights constrained the flare's duration from about 1 d to several weeks.

Flare 1 was the brightest. It was detected on two plates (the rising branch on ac34636 and the peak on bm01044) from the same night (Fig. 5a). However, bm01044 is quality flagged. Our inspection of the field on this plate showed that this flagging could be caused by the elongation of the stars due to inaccurate guiding of the telescope. Nevertheless, a comparison of the image of EI UMa with the surrounding stars in the field showed that this object was brighter than in the nearby nights. Regarding the significance of flare 1 in JD 242 9245.916, the peak magnitude of EI UMa was 12.65 \pm 0.10, and the limiting magnitude of the plate was 14.70. The separation S of the brightness of EI UMa from the limiting magnitude (background) was 2.05 mag, which suggests the significance of the flare about 20σ . The plates surrounding flare 1 constrain its amplitude of 1.6 mag and the duration of at most about 1 d.

Flare 2 was captured on two plates (dnb00870 and dnb00871) from the same night and showing mutually quite similar brightness of EI UMa (Fig. 5a). A detail of the light curve in this flare's surroundings is displayed in Fig. 5(b). Our inspection of the plates revealed that the difference between the brightness of EI UMa and the limiting magnitude of the plates surrounding the flare was bigger for flare 2 than for flare 1. The brightness of EI UMa in flare 2 (JD 244 2388.9) was 13.20 ± 0.11 mag, and the limiting magnitude

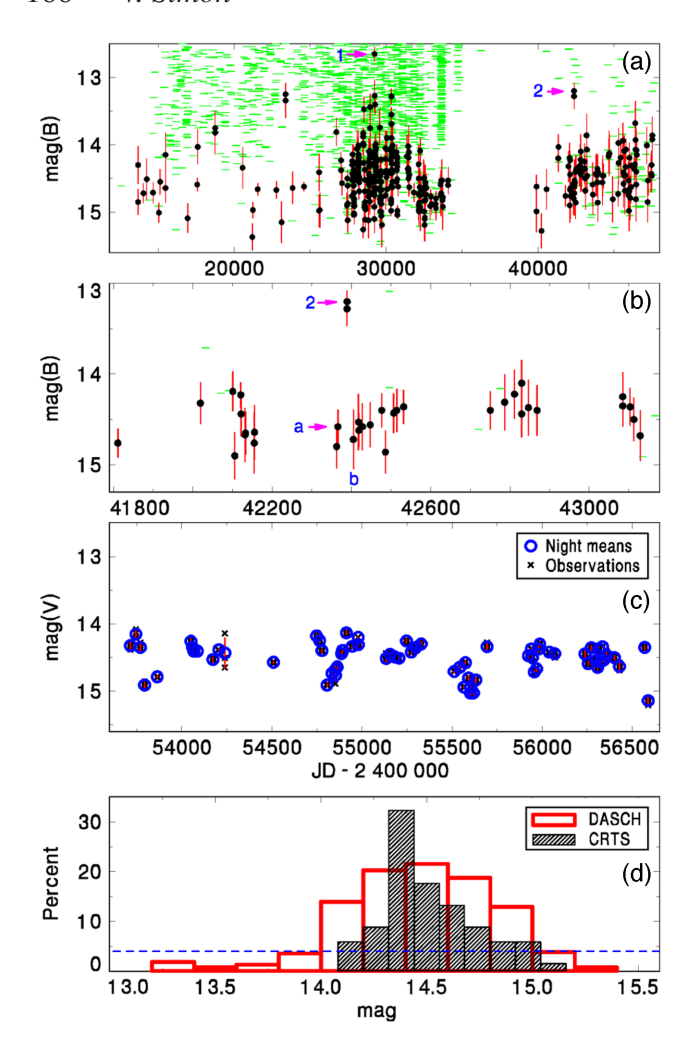


Figure 5. (a) The DASCH long-term light curve (roughly the *B* band) of EI UMa. The errors of brightness, listed in the original data file, are given. Short horizontal green lines represent the upper limits of brightness. (b) Detail of the light curve in the surroundings of flare 2. (c) The CRTS *V*-band light curve. The distances between the ticks on the vertical axis are the same for the panels (a), (b) and (c). (d) Histogram of the brightness of the DASCH observations and the CRTS night means of data. The dashed line represents the level of 4 per cent of observations of a given data set. See Section 3.4 for details.

(background) of the plate was 15.15. The value of $S \approx 1.95 \, \text{mag}$ thus suggests the significance of about 17σ . The surrounding plates (points a and b in Fig. 5) constrained the duration of the flare to be at most about 39 d.

The later CRTS observations (Fig. 5c) showed a series of fluctuations in the time-scale of weeks and months. The amplitudes of these fluctuations were higher than those of intranight variations. No flares were detected. The absence of flares in the CRTS data may be due to a short time segment compared with the previous one covered by the DASCH data.

The histograms of brightness in Fig. 5(d) show the properties of activity consisting of various features (e.g. flares, fluctuations). The bin widths are 0.20 and 0.12 mag for the DASCH and the CRTS observations, respectively. The difference is that a typical error of the DASCH data is bigger than that of the CRTS observations, so only the histogram's main features are meaningful.

Only the histogram for the DASCH data contains a long tail towards a higher brightness, visible below the level of 4 per cent

of observations (i.e. below the dashed line in Fig. 5d). The end of this tail is marked as the diamond in Fig. 1. The width of the bump in Fig. 5(d), measured at this line of 4 per cent of observations (excluding thus the flares detected only in the DASCH data), is similar for both data sets. The brightnesses of the borders of this bump at this level differ by at most about 0.2 mag for both data sets. This bump spans between the square and the circle in Fig. 1.

The values of $M_{\rm opt}$ of EI UMa in Fig. 1 suggest that the luminosity is comparable with the peaks of the outbursts of DNe. The similarities of the bumps in the histograms in Fig. 5(d) along with the high $M_{\rm opt}$ and $B-V\approx 0$ (Reimer et al. 2008) suggest that the accretion disc dominated the optical luminosity of EI UMa and that the contribution of the light of the secondary was negligible. A combination of the histograms for photographic and CCD observations enables us to show that EI UMa is an example of an IP that displays a very high optical luminosity and a high \dot{m} for decades.

In the interpretation, the flares of EI UMa are the bursts of the transferred matter from the donor. The model of Hameury & Lasota (2017) shows that such a burst on to an ionized disc causes an outburst with a slow decay (more than about $10\,\mathrm{d}$) of optical emission. Based on the limits of durations of some flares in the DASCH observations, we cannot exclude the possibility that they are consistent with the decay of an ionized disc. We suggest several solutions for EI UMa. (i) The short flares are the impacts of matter on to a cool disc (so only the impact region of the stream brightens); furthermore, the disc is not ionized even when M_{opt} is close to that of DNe at the peak of the outburst. (ii) A disc overflow of the matter occurred (see Hellier 1993b for a stream impact in FO Aqr). Nevertheless, as regards flare 2, the data gaps do not enable us to resolve a burst of the mass transfer from the donor into a cool or a hot (ionized) disc.

The activity of EI UMa also bears a similarity with another IP, V1062 Tau, which displays both an episode of a shallow low state and rare, short outbursts (Lipkin, Leibowitz & Orio 2004). While $M_{\rm opt}$ of V1062 Tau is well below the peak magnitudes of the outbursts of DNe (fainter than EI UMa), the brightness of its outburst is consistent with that of these peaks.

3.5 HY Leo

HY Leo (HS 0943+1404) is an IP with $P_{sp}/P_{orb} \approx 0.3$, discovered by Rodríguez-Gil et al. (2005). This system enters into deep (about 3 mag) low states, which are a characteristic feature of polars (Rodríguez-Gil et al. 2005). Also, the WD's magnetic moment, estimated to be $\approx 10^{34}$ G cm³, is in the typical range of polars. They suggest that HY Leo will eventually synchronize and that this is an object between IPs and polars.

Rodríguez-Gil et al. (2005) also find that HY Leo displays alternating dominance of the spin and beat signals in the optical light curves. This fact implies changes in the accretion mode. They are not solely due to variations in \dot{m} of HY Leo, but can also be triggered by other mechanisms within the binary (see also Norton et al. 1997). Rodríguez-Gil et al. (2005) argue that the accretion disc must dominate the observed continuum of HY Leo; a predominant signal at the beat period cannot be unambiguously linked to disc-less accretion.

Fig. 6(a) shows the extreme long-term activity of HY Leo with the peak-to-peak amplitude of more than four mags (spanning between the diamond and the square in Fig. 1). The peak-to-peak amplitude of intranight variations is much lower than the amplitude of the long-term variations. The light curve is divided into four segments (S1 to S4) in Fig. 6.

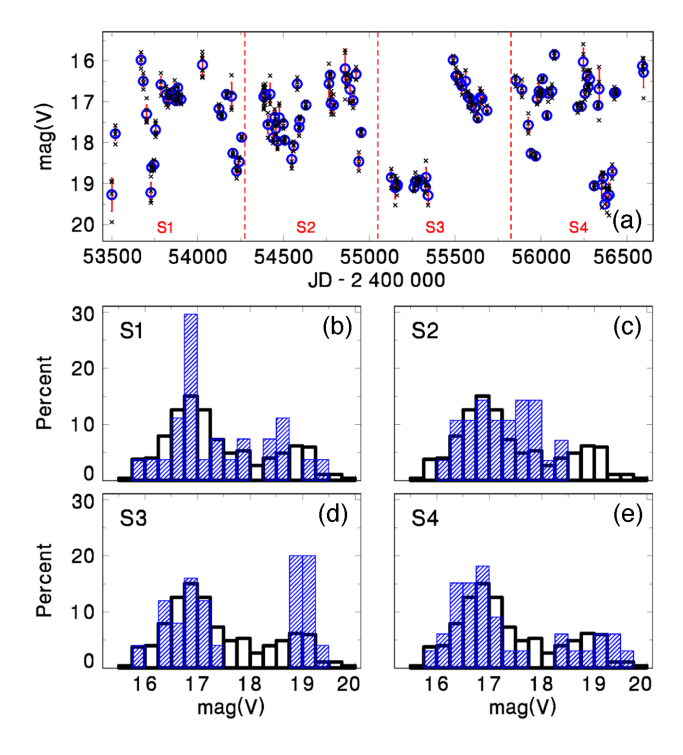


Figure 6. (a) The long-term activity of HY Leo (the CRTS data). Both the observed data (crosses) and the night means (circles) are shown. The vertical lines denote the standard deviations of the means of brightness. The light curve is divided into four segments (S1 to S4). (b)–(e) Histograms of brightness for these segments. The empty bars represent the histogram for the whole data set from panel (a). The shaded bars represent the data for a given time segment. See Section 3.5 for details.

In Figs 6(b)–(e), the histogram of the brightness of the whole data set (the empty bars) from Fig. 6(a) is compared with the data for a given time segment. We attributed a broad bump centred on mag(V) = 16.9 in the histogram for the segments S1–S4 in Fig. 6 to the high state.

A broad bump near mag(V) = 16.9 in Figs 6(b)–(e) shows that the high-state brightness was variable. Its width was not only the result of many high-state episodes with different mean magnitudes. Also, a given high-state episode displayed the fluctuations of brightness on the superorbital time-scale. The very existence of a peak suggests that the optical luminosity tended to return to roughly the same average value in the individual high-state episodes no matter how deep and long the low-state episodes were. The onset of the state transition did not occur at the same brightness for the individual episodes. For example, a slow decay of brightness in the high-state episode (marked 1) in Fig. 7 continued even when other high-state episodes (around JD 245 6250) rapidly finished at a considerably higher luminosity. This fact suggests that the transition's start did not strictly depend on its $M_{\rm opt}$.

Fig. 6 shows several small peaks in the high-state episodes. Although the values of $M_{\rm opt}$ are lower than the peaks of the outbursts of DNe (Fig. 1), the light curve does not correspond to that of the Z Cam-type DNe (see Warner 1995 for an example and description of the Z Cam-type). These high states of HY Leo thus do not correspond to the standstills.

A combination of the light curve with the histograms of brightness showed that the activity of HY Leo could be identified with a series of high and low states, seen in nova-likes (e.g. Honeycutt & Kafka 2004), although the gaps in the data did not enable an accurate

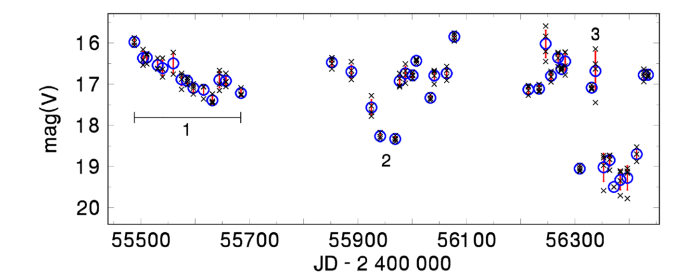


Figure 7. A segment of the light curve of HY Leo from Fig. 6. A long high state (1), a low-state episode (2) and a short brightening (3) are marked. See Section 3.5 for details.

determination of the e-folding time of the transitions. This series of high and low states in HY Leo occurred when $M_{\rm opt}$ resided deep in the region of the TVI (Fig. 1). Therefore, we interpreted its disc as remaining in the cool state in both the high and the low states.

The activity of HY Leo was similar to that of other nova-like IPs, such as V1223 Sgr (Garnavich & Szkody 1988; Šimon 2014), with mutually very different depths of the low-state episodes. We interpreted the state transitions of HY Leo as the episodes of decreases of \dot{m} from the donor to the WD. HY Leo was indeed close to the region of $P_{\rm orb}$ of the VY Scl nova-likes (Hameury & Lasota 2002). The length of $P_{\rm orb}$ of HY Leo is not that different from the polar AM Her (Tapia 1977) that also exhibits low states (e.g. Wu & Kiss 2008).

In the interpretation, the variations of \dot{m} governed the state transitions of HY Leo. The variable depths and lengths of the individual low-state episodes suggest differences in the strength and extension of some active regions on the donor, for example, spots (Livio & Pringle 1994). The returns to roughly the same brightness of the high state speak in favour of the low states caused by the transiently existing active regions. We also ascribed the fluctuations of the high-state brightness to the variations of \dot{m} governed by the processes in the donor.

No DN outbursts were detected in the low-state episodes of HY Leo (Fig. 7). No DN outbursts occurred even during any state transitions. Using the model of Hameury & Lasota (2002), this can be explained by the accretion disc residing in the cool state in both the high and the low states.

As regards the existence of the disc in the deep low states in S3 and S4 (except flare 3 lasting for 7–44 d) in Fig. 7, the value of $M_{\rm opt}$ of HY Leo was comparable with that of DW Cnc (Fig. 1), in which the disc was present (Rodríguez-Gil et al. 2004). Although the light contribution of the donor is expected to be significant in these low states of HY Leo (Fig. 1), the brightness fluctuated on the time-scale of weeks (and even during some nights) by several tenths of mag. Therefore, we observed either an intense activity of a luminous donor or a combination of the light from the donor and the remaining matter in the lobe of the WD.

We can compare this with the situation of another IP, FO Aqr, in the low state (Kennedy et al. 2020). A decrease in its brightness in the low state was coupled with a change of the accretion structures; a combination of disc-fed and ballistic stream-fed accretion was present. The disc, therefore, did not disappear in this low state.

We ascribe flare 3 in HY Leo to a burst of mass outflow from the donor. Before and after this flare, the mutually similar brightnesses suggest that the matter from this burst had to dissipate (or accrete) during less than 15 d. In the interpretation, the flare emission came from the hotspot where the inflowing stream collided with such a

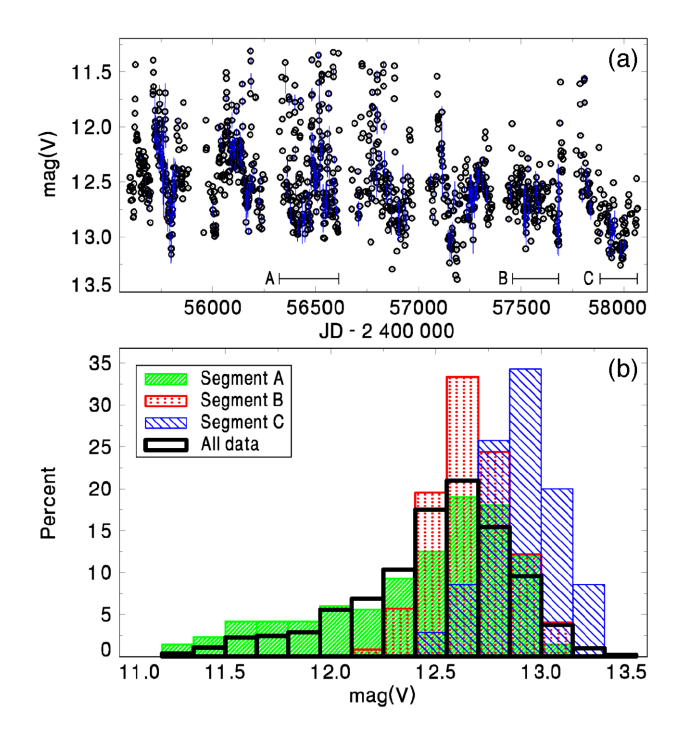


Figure 8. (a) The long-term light curve of V426 Oph (the AAVSO CCD *V*-band 1-d means). The vertical lines mark the standard deviations of the brightness of the night means. Segments A, B and C are marked. (b) Histograms of brightness. The histograms for the individual segments are compared with those for the whole data set. See Section 3.6 for details.

cool disc or a torus (the model of Hameury & Lasota 2017), still existing in this low state.

3.6 V426 Oph

V426 Oph stands out with exceptionally hard X-ray spectral distribution of *ASCA* GIS hardness ratios of various CVs by Baskill et al. (2005). They argue that it should be reclassified as an IP based on this spectral property. They also argue that the X-ray spectra of V426 Oph and EI UMa represent excellent evidence for magnetically confined accretion on to the WD.

V426 Oph displayed modulation in X-rays: 2.5 and 4.5 h (Rosen et al. 1994), 0.467 h (Szkody, Kii & Osaki 1990), 2.1 and 4.2 hr (Homer et al. 2004) and 0.4867 h (Baskill et al. 2005). However, the later analysis of Ramsay et al. (2008) showed that the X-ray modulations were transient, and their frequency was not stable. According to Ramsay et al. (2008), V426 Oph does not show evidence for a spin period because it has closely aligned magnetic and spin axes. It shows complex and high absorption of X-ray emission, characteristic of IPs. Therefore, they believe that it is a bona fide IP. Hessman (1988) shows that although the behaviour of the emission lines is complex, the broad, double-peaked emission-line profiles expected from a simple, rotating disc are often seen, indicating that a disc fills about 70 per cent of the Roche lobe.

Shafter, Cannizzo & Waagen (2005) show that the series of outbursts of V426 Oph shares some characteristics with the ensemble of the Z Cam DNe. Nevertheless, it displays a considerably larger scatter of the recurrence times $T_{\rm C}$ of these events.

The light curve consisting of a dense series of the 1-d means of the AAVSO CCD observations of V426 Oph is shown in Figs 8 and 9. These means were used because the number of observations was very different for the individual nights. This approach enabled us to make unbiased histograms of brightness. Episodes of brightening

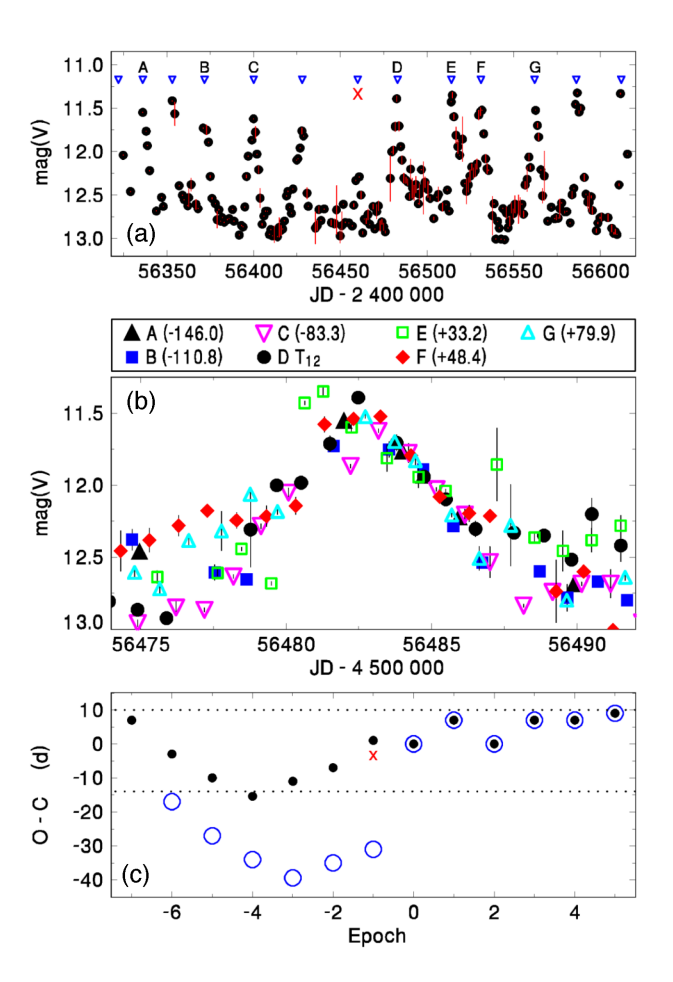


Figure 9. (a) A detail of the light curve of V426 Oph in segment A. The triangles mark peaks of the outbursts. (b) Light curves of the well-observed outbursts, folded along their decaying branch. These outbursts are identified in panel (a). Outburst D is the template, T_{12} is the time of crossing mag(V) = 12 on the decaying branch. The numbers in brackets refer to the time intervals in days between a given outburst and the template. (c) The O – C diagram of $T_{\rm C}$ of the outbursts from panel (a). The ephemeris is given in equation (1). The solid black circles represent the O – C curve, which includes the outburst abbreviated as X in panels (a) and (c). The open blue circles denote the O – C curve without X. See Section 3.6 for details.

(outbursts) represent a large part of the brightness variations. Also, several shallow low states such as the one around JD 245 7950 were present.

Folding the dense series of the CCD V-band data (Kafka 2018), obtained in some nights, with $P_{\rm orb}$ according to the ephemeris of Hessman (1988) only revealed non-periodic fluctuations on the timescales of tenths of $P_{\rm orb}$. They were similar to those in Hellier et al. (1990). We found that their profile and the peak-to-peak amplitude varied for the individual nights even when the brightness, averaged over $P_{\rm orb}$, remained similar. These variations were not related to the orbital phase. Thus, they could not be identified either with a hotspot in the stream—disc interaction region, spin modulation or irradiation of the donor

The histograms of brightness are displayed in Fig. 8(b). A single bump of the whole data set (spanning between the square and the circle in Fig. 1) represents an extensive quiescent level (between the brightenings). It gradually transitions to a tail, consisting of the brightenings (outbursts), present mainly in segment A. Their brightest peak represents a diamond in Fig. 1. Segment B is an example of the time in which the brightenings (outbursts) are absent,

although the brightness is compatible with the quiescence between the brightenings observed in segment A (Figs 8a and 8b). Segment C represents a shallow low state. This feature represents a faint tail of the histogram of the whole data set.

The light curves of the well-observed brightenings (outbursts) were folded along their decaying branches (Fig. 9b). Outburst D, identified in Fig. 9(a), was the template. The time of crossing mag(V) = 12 of the decaying branches of the individual outbursts was used for determining the time shifts with respect to the template. We found that the outbursts' decay rates in Fig. 9(b) were mutually similar. The decay rate of the DN outburst, τ_D , expressed in days for a decrease in brightness of 1 mag (Bailey 1975), enables us to assess how much a given outburst obeys the Bailey relation (Bailey 1975). We compared the outbursts of V426 Oph to an ensemble of the DN outbursts in Warner (1995). We thus found that they obeyed the Bailey relation. The values of $M_{\rm opt}$ place V426 Oph in the region of CVs fainter than the peaks of the outbursts of DNe (Fig. 1). All this speaks in favour of the TVI of the disc.

In the model for DNe, this decay is governed by the propagation of the cooling front (Smak 1984; Hameury et al. 1998). The slope of this decay was found to be very similar for the individual events of a given DN, for example, SS Cyg (Cannizzo & Mattei 1998), DO Dra (Šimon 2000a), DX And (Šimon 2000b) and GK Per (Šimon 2002). The scatter of the light curves of the rising branches can vary for the individual DNe. It was enormous for DX And (Šimon 2000b), interpreted as a heating front starting in various distances from the WD, r_s , for the individual outbursts. In the interpretation, the values of r_s were almost the same for the individual outbursts of V426 Oph.

While the outbursts are longer for DNe (presumably non-magnetic) with longer $P_{\rm orb}$, and a given DN often displays alternating outbursts of two groups according to their length (van Paradijs 1983), the outbursts of V426 Oph belong to only one group. In this interpretation, the sharp peaks suggest the absence of the viscous plateau (Hameury et al. 1998).

Because the outbursts in segment A (Fig. 9a) are the discrete events with easily resolvable peaks, the method of the O-C residuals of some reference period is suitable for an analysis of their T_C ('O' stands for observed and 'C' for calculated times). Vogt (1980) applied this method to several DNe.

Minimizing the slope of the O – C values generated for various $T_{\rm C}$ yielded $T_{\rm Cref}$, the reference value of $T_{\rm C}$. The resulting ephemeris is given by

$$t_{\text{max}} = T_{\text{b}} + T_{\text{Cref}}E,\tag{1}$$

where the time of the basic peak of outburst, $T_{\rm b}$, is equal to JD 245 6483, $T_{\rm Cref}$ is equal to 24 d and E is epoch.

Fig. 9(c) shows that although the length of $T_{\rm C}$ in segment A was variable, the occurrence of these outbursts was not dramatically irregular. The outburst abbreviated as X in Fig. 9 was fainter and shorter than other outbursts. Therefore, we investigated whether it was an outburst or only a fluctuation of the quiescent brightness between the outbursts. We found that the outburst position X was consistent with the O-C curve defined by other outbursts in Fig. 9(c). Although the O-C curve without outburst X had a higher amplitude, its profile remained similar.

The scatter of the O-C values of the neighbouring (or nearby) outbursts was considerably smaller than the amplitude of the whole O-C curve. This speaks in favour of the individual outbursts dependent on each other, although the peak magnitude of the outburst was not related to the current length of T_C .

In the TVI model (Smak 1984; Hameury et al. 1998), only a small part of the disc matter is accreted in outbursts while a large

part remains in the disc. The TVI can explain the O-C curve of V426 Oph with the outbursts dependent on each other.

The borders of the series of outbursts in V426 Oph were relatively sharp. In the interpretation, this cool disc was close to switching to the hot state. A small increase of the mass inflow to the disc could give rise to an increase in the column density of the disc, leading to the repeated transitions of the disc from the cool to the hot state (see the model of Lasota et al. 1995). The absence of outbursts did not need to lead to the change of brightness of the quiescent state. The bump made of the magnitudes in segment B in Fig. 8 was similar to that of the bump of segment A for mag(V) lower than 12.3.

No DN outbursts occurred when V426 Oph was in a shallow low state (in the surroundings of JD 245 7950). The different peak magnitudes of the individual outbursts suggest that the duration of the quiescent interval (before or after the outburst) was mostly independent of the amount of the radiated energy of a given outburst in the optical band. We ascribe the variations of brightness of the quiescent state to the cool disc. The depth of this low state was diminished by the fact that V426 Oph became only about 0.5 mag brighter than the donor.

The activity of V426 Oph does not correspond to that of the Z Cam DNe described by Warner (1995). The reason is that the time segments of the light curve with the missing outbursts do not correspond to such systems' standstills. Although the optical luminosity of the standstills in the Z Cam DNe is lower than the peaks of their outbursts, it is considerably higher than the quiescence.

4 DISCUSSION AND CONCLUSION

This analysis of the long-term optical activity of five examples of IPs containing accretion discs shows that they occur in an extensive range of optical luminosity. We found that $M_{\rm opt}$ of each of these IPs has its most preferred value(s) even if it significantly varies on the superorbital time-scales. The long-term optical activity consists of discrete features (flares, outbursts, state transitions). In the interpretation, it depends on the mean mass inflow rate to the disc from the donor in a given IP.

The luminosity of the accretion disc dominates because $M_{\rm opt}$ of each of these IPs is significantly higher than that of the secondary component (with a possible exception of the deepest low states of HY Leo and V426 Oph). This suggests that a significant scatter of $M_{\rm opt}$ of IPs is caused by the very different luminosities of their accretion discs. As none of these IPs displays deep eclipses, this indicates that they are not observed as very close to their orbital plane. Thus, their inclination plays only a minor role in this scatter of $M_{\rm opt}$.

The values of $M_{\rm opt}$ of IPs in Fig. 1 show that these systems spend the most time with optical luminosity lower than that of the peaks of the outbursts of the presumably non-magnetic DNe. Although the values of $M_{\rm opt}$ of IPs in Fig. 1 speak in favour of the accretion discs in the region of the TVI, the outbursts of most of them are rare, and their amplitudes are lower than in non-magnetic DNe. Some IPs can reside without the DN outbursts at these luminosities for years. Not all their detected outbursts may even be caused by the TVI.

Although the typical values of $M_{\rm opt}$ of V426 Oph and TV Col are mutually similar and lie in the region in which the TVI of the disc should be present, the activities of both IPs are different from each other because a series of DN outbursts is present only in V426 Oph. In the interpretation, this series of the DN outbursts suggests an intermittently operating TVI of the disc, which occurs if a mass inflow from the donor transiently increases the column density of the matter of the disc. The condition for the TVI of the disc to occur is that the mass transfer rate has to be low enough that the disc cannot be

170 *V. Šimon*

permanently in the high state and high enough that it cannot be stable in the low state. The difference between the activity of V426 Oph and TV Col is caused by a larger Alfvén radius in TV Col, which keeps the disc in the cool state all the time; thus, only the bursts of the mass outflow from the donor (but not the TVI of the disc) cause variations in its luminosity.

Both TV Col and DW Cnc (although the lengths of their $P_{\rm orb}$ are considerably different from each other) show a gradual evolution of brightness on the time-scale of hundreds of days, with the short flares superimposed on them. In the interpretation, both TV Col and DW Cnc possess discs in the cool state with a very low viscosity. The changes of \dot{m} from the donor to the disc governed their gradual brightness variations on the time-scales of months. The mass transfer rate from the secondary varies on a well-determined time-scale. We ascribe the big outburst (Crawford et al. 2008) in DW Cnc to a TVI event when \dot{m} was large.

Fig. 1 shows that one of these IPs, EI UMa, almost reaches the luminosity of the peaks of the DN outbursts for decades. In the interpretation, keeping the high $M_{\rm opt}$ for a long time is achieved by a sufficiently high \dot{m} , comparable to that in non-magnetic nova-likes.

EI UMa, TV Col and DW Cnc with mutually different $P_{\rm orb}$ and $M_{\rm opt}$ possess short outbursts (flares). The low peak-to-peak amplitudes of their flares (1–1.5 mag) are consistent with those of stunted outbursts (Honeycutt, Robertson & Turner 1998; Honeycutt 2001). Honeycutt (2001) investigated an ensemble of CVs and showed that most CVs with stunted outbursts are old novae and nova-likes with high $M_{\rm opt}$. He argued in favour of the TVI as the cause of stunted outbursts, with the contribution of an extra source of the light variable in strength from system to system.

In this context, a comparison of EI UMa, TV Col and DW Cnc shows that optical luminosities of the flares increase with increasing quiescent $M_{\rm opt}$ in these three IPs. Several processes might generate stunted outbursts in various CVs. The short duration of the flares and their amplitudes concerning the quiescent brightness, only barely dependent on the quiescent $M_{\rm opt}$, speak in favour of the bursts of matter from the donor (the model of Hameury & Lasota 2017). Although the spectra of these flares are very rare, the observations of Hellier & Buckley (1993) suggest that one of them in TV Col was caused by a burst of the mass transfer from the donor.

The activity of HY Leo, with the rapid transitions to deep low states, shows that these transitions can occur even in IPs that contain cool discs all the time. This behaviour bears a similarity with another IP, V1223 Sgr (Garnavich & Szkody 1988; Šimon 2014). The high states of HY Leo (and similarly in V1223 Sgr; Šimon 2014) are not any uniquely defined levels of brightness. In the histograms of brightness, the low states sometimes represent the tails from such broad bumps rather than the specific brightness levels. The fuzzy boundaries of the bright side of the histogram of brightness show that the system cannot find the stability of the mass transfer even in the high state. We ascribe the long-term brightness variations of these IPs to the donor's activity, which causes the largely variable mass inflow rate into the disc.

For comparison, another IP, DO Dra, with $P_{\rm orb}=3.96\,{\rm h}$ (similar to $P_{\rm orb}$ of the systems in our study; Mateo, Szkody & Garnavich 1991) and $P_{\rm sp}=0.147\,{\rm h}$ (Haswell et al. 1997; Patterson et al. 1992), is an extreme case as regards the TVI because it resides in a very low quiescent luminosity with a low mass inflow rate to the WD, $\dot{m}_{\rm WD}$ (Dubus, Otulakowska-Hypka & Lasota 2018). It displays rare, intense outbursts, which can be explained by the TVI (e.g. Patterson et al. 1992; Šimon 2000a; Szkody et al. 2002; Andronov et al. 2008). Szkody et al. (2002) and Patterson & Szkody (1993) argue in favour of a peculiar geometry, combined with the poles' locations in the equatorial plane of the WD. Norton et al. (1999) argue in favour of a

weak magnetic field of the WD so that the disruption radius is small. All of this can influence the occurrence of the TVI. As regards the large variety of the long-term changes of $M_{\rm opt}$ of IPs, a long $P_{\rm orb}$, hence a big radius of the accretion disc in the IP GK Per (Watson, King & Osborne 1985) with $P_{\rm orb}$ of 47.76 h (Crampton, Cowley & Fisher 1986), gives rise to the large-amplitude DN outbursts with the duration of weeks, ascribed to the TVI (Hudec 1981; Sabbadin & Bianchini 1983; Kim, Wheeler & Mineshige 1992; Šimon 2002). They are similar to those in the non-magnetic DNe, so the magnetic field of the WD is not able to dramatically modify the TVI of the disc of some IPs. In conclusion, the long-term activity properties and features can help assess the mass transfer properties in IPs.

The range of $M_{\rm opt}$ of IPs in our study falls into that of $M_{\rm opt}$ of nCVs (except outbursts of classical novae; see, e.g. Warner 1995). However, the activity of these IPs on the time-scale from days to years is different from that of nCVs.

The type of long-term activity of nCVs depends on the time-averaged mass transfer rate between the components, $\dot{m}_{\rm av}$. The value of $\dot{m}_{\rm av}$ plays a significant role in a sequence of types of nCVs.

If the value of $m_{\rm av}$ of a given nCV is between some limits, the accretion disc is exposed to the TVI, which manifests as outbursts with a typical amplitude of about 2–5 mag (Smak 1984; Hameury et al. 1998). Warner (1987, 1995) showed that the DN outbursts play a big role in the activity of many nCVs. The values of $M_{\rm opt}$ of the peaks of the DN outbursts, in which the disc becomes ionized out to its outer rim, gradually increase with an increasing $P_{\rm orb}$ (e.g. Warner 1987; Patterson 2011; see Fig. 1). Quiescent DNe accumulate between $M_{\rm opt}$ about 9.5 and 7 for $P_{\rm orb}$ about 1.5–7 h (the IPs in our study are brighter than these values of $M_{\rm opt}$).

A higher $\dot{m}_{\rm av}$ of nCVs in the TVI region is predicted to lead to a higher time-averaged optical luminosity. It also leads to a shorter $T_{\rm C}$ of DNe if $\dot{m}_{\rm av}$ is high enough that the outburst can be of the outside-in type (Smak 1984; Hameury et al. 1998). However, although the IPs in this study display different time-averaged optical luminosities, a higher value does not lead to more numerous DN outbursts. Most of them usually do not display the DN outbursts at all and reside in various $M_{\rm opt}$ in their low states.

The high states of non-magnetic nova-likes in which no outbursts occur have a high $M_{\rm opt}$, comparable with that of the DN outbursts or even higher (Warner 1987). Their accretion discs are supposed to be in the hot state (Warner 1995). However, the missing DN outbursts at various values of $M_{\rm opt}$ of most IPs in our study do not enable us to resolve whether they are DN in the quiescent state or nova-likes.

Therefore, we can conclude that the IPs in our study reside between $M_{\rm opt}$ of quiescent and outbursting non-magnetic DNe. However, they do not fall into the sequence of nCVs mentioned above. The amplitude of the outbursts of non-magnetic DNe is considerably higher than that of the outbursts (flares) of IPs in our study. Also, the DN outburst length of non-magnetic DNe (Ak, Ozkan & Mattei 2002) is more prominent than in IPs.

Only nCVs with the time-averaged $M_{\rm opt}$ close to DNe at the peaks of outbursts become nova-likes (Warner 1995) while the IPs in our study reside with no or a very few such DN outbursts for years, even in the region of the TVI of nCVs in Fig. 1. Perhaps a smaller disruption radius could enable the DN outbursts in IPs. Also, a bigger radius of the disc is an alternative.

ACKNOWLEDGEMENTS

This study was supported by the EU project H2020 AHEAD2020, grant agreement 871158, and project RVO:67985815. This research has made use of observations from the DASCH project at Harvard, partially supported by National Science Foundation grants AST-

0407380, AST-0909073 and AST-1313370. This work also used data from the Catalina Transient Survey, the AAVSO International Data base (USA), and the AFOEV data base (France). I thank variable star observers worldwide. I acknowledge using the 3D reddening map constructed by Green et al. (2018) (http://argonaut.skymaps.info). I also thank Professor Petr Harmanec for providing me with the code HEC13. The Fortran source version, compiled version, and brief instructions on how to use the program can be obtained at http://astro.troja.mff.cuni.cz/ftp/hec/HEC13/.

DATA AVAILABILITY

The data sets were derived from sources in the public domains.

REFERENCES

Ak T., Ozkan M. T., Mattei J. A., 2002, A&A, 389, 478

Andronov I. L., Chinarova L. L., Han W., Kim Y., Yoon J-N., 2008, A&A, 486, 855

Augusteijn T., Heemskerk M. H. M., Zwarthoed G. A. A., van Paradijs J., 1994, A&AS, 107, 219

Bailer-Jones C. A. L., Rybizki J., Fouesneau M., Mantelet G., Andrae R., 2018, AJ, 156, 58

Bailey J., 1975, J. Brit. Astron. Assoc., 86, 30

Baskill D. S., Wheatley P. J., Osborne J. P., 2005, MNRAS, 357, 626

Brockwell P. J., Davis R. A., 1987, Time Series: Theory and Methods. Springer, Berlin

Brown R. A. G. A.et al. (Gaia Collaboration), 2018, A&A, 616, A1

Buckley D. A. H., Sekiguchi K., Motch C., O'Donoghue D., Chen A-L., Schwarzenberg-Czerny A., Pietsch W., Harrop-Allin M. K., 1995, MNRAS, 275, 1028

Cannizzo J. K., Mattei J. A., 1998, ApJ, 505, 344

Crampton D., Cowley A. P., Fisher W. A., 1986, ApJ, 300, 788

Crawford T., Boyd D., Gualdoni C., Gomez T., MacDonald W. II, Oksanen A., 2008, JAVSO, 36, 60

Cropper M., 1990, Space Sci. Rev., 54, 195

Drake A. J. et al., 2009, ApJ, 696, 870

Dubus G., Otulakowska-Hypka M., Lasota J.-P., 2018, A&A, 617, A26

Garnavich P., Szkody P., 1988, PASP, 100, 1522

Green G. M. et al., 2018, MNRAS, 478, 651

Grindlay J., Tang S., Los E., Servillat M., 2012, Proc. IAU Symp. Vol. 285, New Horizons in Time-Domain Astronomy. Kluwer, Dordrecht, p. 29

Grindlay J. E., Griffin R. E., 2012, Proc. IAU Symp. Vol. 285, New Horizons in Time-Domain Astronomy, Kluwer, Dordrecht, p. 243

Hameury J.-M., Lasota J.-P., 2002, A&A, 394, 231

Hameury J.-M., Lasota J.-P., 2017, A&A, 602, A102

Hameury J.-M., Menou K., Dubus G., Lasota J.-P., Hure J.-M., 1998, MNRAS, 298, 1048

Harmanec P., 1992, the code hec13. Available at: http://astro.troja.mff.cuni.c z/ftp/hec/HEC13/

Haswell C. A., Patterson J., Thorstensen J. R., Hellier C., Skillman D. R., 1997, ApJ, 476, 847

Hellier C., 1993a, MNRAS, 264, 132

Hellier C., 1993b, MNRAS, 265, L35

Hellier C., Beardmore A. P., 2002, MNRAS, 331, 407

Hellier C., Buckley D. A. H., 1993, MNRAS, 265, 766

Hellier C., O'Donoghue D., Buckley D., Norton A., 1990, MNRAS, 242, 32

Hessman F. V., 1988, A&AS, 72, 515

Hessman F. V., Gänsicke B. T., Mattei J. A., 2000, A&A, 361, 952

Homer L. et al., 2004, ApJ, 610, 991

Honeycutt R. K., 2001, PASP, 113, 473

Honeycutt R. K., Kafka S., 2004, AJ, 128, 1279

Honeycutt R. K., Robertson J. W., Turner G. W., 1998, AJ, 115, 2527

Hudec R., 1981, Bull. Astron. Inst. Czechosl., 32, 93

Hudec R., Šimon V., Skalický J., 2005, ASPC, 330, 405

Hutchings J. B., Crampton D., Cowley A. P., Thorstensen J. R., Charles P. A., 1981, ApJ, 249, 680

 $Kafka\ S., 2018, Observation\ from\ the\ AAVSO\ Int.\ Database, \\ {\color{blue}www.aavso.org}$

Kafka S., Honeycutt R. K., 2005, AJ, 130, 742

Kennedy M. R. et al., 2020, MNRAS, 495, 4445

Kim S-W., Wheeler J. C., Mineshige S., 1992, ApJ, 384, 269

Kozhevnikov V. P., 2010, Astron. Lett., 36, 554

Krzeminski W., Serkowski K., 1977, ApJ, 216, L45

Kuulkers E., Norton A., Schwope A., Warner B., 2006, in Lewin W., van der Klis M., eds, Compact Stellar X-ray Sources, Cambridge Astrophysics Series, No. 39. Cambridge University Press, Cambridge, p. 421

Lasota J. P., Hameury J. M., Hure J. M., 1995, A&A, 302, L29

Lipkin Y. M., Leibowitz E. M., Orio M., 2004, MNRAS, 349, 1323

Livio M., Pringle J. E., 1994, ApJ, 427, 956

Mateo M., Szkody P., Garnavich P., 1991, ApJ, 370, 370

Norton A. J., 1993, MNRAS, 265, 316

Norton A. J., Beardmore A. P., Allan A., Hellier C., 1999, A&A, 347, 203

Norton A. J., Hellier C., Beardmore A. P., Wheatley P. J., Osborne J. P., Taylor P., 1997, MNRAS, 289, 362

Norton A. J., Watson M. G., 1989, MNRAS, 237, 853

Nucita A. A., Conversi L., Licchelli D., 2019, MNRAS, 484, 3119

Pandel D., 2004, PhD thesis, University of California, Santa Barbara

Patterson J., 1979, ApJ, 234, 978

Patterson J., 2011, MNRAS, 411, 2695

Patterson J., Price C. M., 1981, ApJ, 243, L83

Patterson J., Schwartz D. A., Pye J. P., Blair W. P., Williams G. A., Caillault J.-P., 1992, ApJ, 392, 233

Patterson J., Szkody P., 1993, PASP, 105, 1116

Patterson J. et al., 2004, PASP, 116, 516

Ramsay G., Wheatley P. J., Norton A. J., Hakala P., Baskill D., 2008, MNRAS, 387, 1157

Rana V. R., Singh K. P., Schlegel E. M., Barrett P., 2004, AJ, 127, 489

Reimer T. W., Welsh W. F., Mukai K., Ringwald F. A., 2008, ApJ, 678, 376 Retter A., Hellier C., Augusteijn T., Naylor T., Bedding T. R., Bembrick C.,

McCormick J., Velthuis F., 2003, MNRAS, 340, 679

Rodríguez-Gil P., Gänsicke B. T., Araujo-Betancor S., Casares J., 2004, MNRAS, 349, 367

Rodríguez-Gil P. et al., 2005, A&A, 440, 701

Rosen S. R., Clayton K. L., Osborne J. P., McGale P. A., 1994, MNRAS, 269, 913

Sabbadin F., Bianchini A., 1983, A&AS, 54, 393

Schrijver J., Brinkman A. C., van der Woerd H., Watson M. G., King A. R., van Paradijs J., van der Klis M., 1985, SSRv, 40, 121

Schwarz H. E., Heemskerk M. H. M., 1987, Proc. IAU Circ., 4508,

Segura M. O., Ramírez S. H., Echevarría J., 2020, MNRAS, 494, 4110

Shafter A. W., Cannizzo J. K., Waagen E. O., 2005, PASP, 117, 931

Smak J., 1984, Acta Astron., 34, 161

Stepanyan D. A., 1982, Perem. Zvezdy, 21, 691

Szkody P., Kii T., Osaki Y., 1990, AJ, 100, 546

Szkody P., Mateo M., 1984, ApJ, 280, 729

Szkody P. et al., 2002, AJ, 123, 413

Šimon V., 2000a, A&A, 360, 627

Šimon V., 2000b, A&A, 364, 694

Šimon V., 2002, A&A, 382, 910

Šimon V., 2014, New Astron., 33, 44

Šimon V., 2015, Proceedings of Science, 022, https://pos.sissa.it/cgi-bin/reader/conf.cgi?confid=255

Tapia S., 1977, ApJ, 212, L125

Thorstensen J. R., 1986, AJ, 91, 940

Uemura M., Kato T., Ishioka R., Novak R., Pietz J., 2002, PASJ, 54, 299

van Paradijs J., 1983, A&A, 125, L16

van Paradijs J., Kraakman H., van Amerongen S., 1989, A&AS, 79, 205

Vogt N., 1980, A&A, 88, 66

Vondrák J., 1969, Bull. Astron. Inst. Czechosl., 20, 349

Warner B., 1987, MNRAS, 227, 23

Warner B., 1995, Cataclysmic Variable Stars. Cambridge Univ. Press, Cambridge

Warner B., McGraw J. T., 1981, MNRAS, 196, 59

Watson M. G., King A. R., Osborne J., 1985, MNRAS, 212, 917

Wu K., Kiss L. L., 2008, A&A, 481, 433

This paper has been typeset from a TEX/LATEX file prepared by the author.